Estimating the Raman cross sections of single carbon nanotubes

Johanna E. Bohn,[†] Pablo G. Etchegoin,[*,†] Eric C. Le Ru,[†] Rong Xiang,[‡] Shohei Chiashi,[‡] and Shigeo Maruyama[*,‡]

The MacDiarmid Institute for Advanced Materials and Nanotechnology, School of Chemical and Physical Sciences, Victoria University of Wellington, PO Box 600, Wellington, New Zealand., and Department of Mechanical Engineering, The University of Tokyo,7-3-1 Hongo, Bunkyo-ku, Tokyo, Japan.

E-mail: pablo.etchegoin@vuw.ac.nz; maruyama@photon.t.u-tokyo.ac.jp

Abstract

The order of magnitude of Raman differential cross sections of radial breathing modes (RBM's) of individual carbon nanotubes is measured for 633 and 785 nm laser excitations, respectively. This is shown by both: a calibration applied to previously published data from other authors at 785 nm, and our own measurements of individual nanotubes at 633 nm excitation. We find typical values of differential cross sections of RBM's to be of the order of $\sim 10^{-22}\,\mathrm{cm}^2/\mathrm{sr}$ for resonant nanotubes on a silicon substrate. This study therefore provides a rigorous quantification of the accepted view that Raman cross-section of carbon nanotubes are "huge".

[†]The MacDiarmid Institute for Advanced Materials and Nanotechnology, School of Chemical and Physical Sciences, Victoria University of Wellington, PO Box 600, Wellington, New Zealand.

[‡]Department of Mechanical Engineering, The University of Tokyo,7-3-1 Hongo, Bunkyo-ku, Tokyo, Japan.

The study of carbon nanotubes and related compounds has intensified in the last few years,[1–3] mainly driven by the prospects of using their unique electronic, mechanical, and optical properties in a variety of nanotechnology frameworks. Since their discovery,[4] Raman spectroscopy[5] has played a leading role in our current understanding of carbon nanotubes,[6,7] and has led to the elucidation of a great variety of phenomena; from the characterization of nanotubes according to their radial breathing mode (RBM) frequencies,[8] to the study of double-resonance phenomena,[9] or "anomalous" anti-Stokes spectra.[10] Studies have also been extended to the realms of Surface-Enhanced Raman Spectroscopy (SERS).[11]

Notwithstanding, there are still (surprisingly) very basic aspects of Raman scattering of carbon nanotubes that have *not* yet been explored. One such example is the experimental estimation of the *differential Raman scattering cross sections* $(d\sigma/d\Omega)$ for differing Raman modes (Radial Breathing Modes (RBMs), *G*-bands, *D*-bands, etc. . .) of different types of nanotubes (semiconducting or metallic; characterized by their chirality indices (n,m)[12]). While a considerable fraction of papers in the topic mention the apparent "huge resonant Raman cross sections" that nanotubes have, a direct attempt to quantify them –even with intrinsic experimental limitations– has not yet been provided in the literature (to the very best of our knowledge). Hence, this letter is aimed directly at filling what we perceive as a gap in the literature: i.e. a direct experimental estimation of differential Raman cross sections of nanotubes, together with the development of a practical protocol that can be followed subsequently by other authors to quantify their observations. The importance of having a reliable estimation of the differential Raman cross sections of nanotubes is, we believe, beyond doubt. This stems not only from the viewpoint that the $d\sigma/d\Omega$'s of nanotubes represent one of their fundamental physical properties but –in addition– from the fact that a proper estimation of Raman differential cross sections might start closing the circle into a whole variety of related phenomena that have been already observed (like the anomalous magnitude of anti-Stokes spectra,[8,10] or the possibility of vibrational pumping).

The main problem with the estimation of Raman differential cross sections in general is to know *how many molecules are contributing to the signal*. While this is not a major problem

for measurements done in transparent liquids of known density and molecular weight (where we can clearly define how many molecules are producing the signal in the scattering volume) it is a daunting task in samples with more complicated characteristics (like forests of nanotubes,[13,14] for example); in particular, if resonance effects produce signals that come from a sub-population of the molecules that are actually in the scattering volume. A non-uniform sample like a forest of nanotubes on a substrate presents a challenging experimental problem, simply because it is not easy to normalize the signal by the number of tubes that are contributing to it. The addition of resonance phenomena only exacerbates the problem. A similar situation occurs, in fact, in SERS, where the inhomogeneity of the enhancement factor makes it very difficult (in general) to estimate how many molecules are contributing to the signal.[15,16] In this case, there is normally no other option but to try to observe *one* molecule (nanotube) at a time.[17] In this latter situation, the difficulty of estimating how many molecules are producing the signal is replaced by the experimental difficulty of finding a way to ensure that (indeed) single molecules are being measured. To this we have to add the experimental limitation that the cross section itself (intrinsic, or enhanced in the case of SERS) has to be large enough to make single molecule (nanotube) observation possible. Fortunately nanotubes fall into this category, without a need for further enhancement of the cross section (like SERS).

Nanotubes are unlike any other normal case of Raman cross section determination for other (smaller) molecules. The fact that some nanotubes can be *longer* than a typical laser spot size ($\sim 0.5-1\,\mu$m at high magnifications) is an indication of how unusual their case is. A few peculiarities of the nanotube problem that are relevant for the forthcoming discussion can be introduced at this stage:

- Nanotubes provide a natural spectroscopic fingerprint to decide single-nanotube detection through their radial breathing modes (RBM's), which –for a specific nanotube– is a signature of its uniqueness among a certain inhomogeneous population of tubes. After Ref.,[12] the measurement of individual RBM's in samples with a low surface coverage (within the area defined by the laser spot) provides a natural mechanism for the identification of single-

nanotubes. In short, the detection of individual nanotubes is ensured by the combination of: (i) samples with low surface density of tubes, and (ii) the additional "resonance selection" by which only tubes with certain characteristics can effectively couple to a particular laser excitation.

- The Raman signals of nanotubes are typically highly polarized.[18] However, exactly as in Ref.,[12] we do not have an easy way of controlling the relative orientation of different nanotubes with respect to the incident polarization. Nanotubes are detected by spatial Raman mappings on a substrate (Si). We therefore expect that the largest values of the differential cross sections obtained in single nanotubes will be (statistically speaking) representative of the largest component of the Raman tensor (when it is aligned accidentally in the right direction). The experimentally obtained values for $d\sigma/d\Omega$ need to be understood in that context.

- A similar proviso holds for the *length* of the nanotube. We cannot easily measure the actual length and the exact spatial position on an individual nanotube within the laser spot (simultaneously with the Raman spectrum itself). Nanotubes are rather large "molecules" with varying lengths in the typical range $\sim 100-300\,\mathrm{nm}$ (according to our SEM images); other authors[12] have grown even larger nanotubes ($\sim 1\mu\mathrm{m}$). If we had the same type of nanotubes (defined by the chirality indices (n,m)) in resonance with the laser under the microscope all the time, and in the same position and orientation with respect to the laser polarization, there will still be a spread of signals caused by their intrinsic variability in length. As with the previous point, the experimentally obtained values have to be interpreted in that context. As we shall explain later, we perform experiments with the minimum laser spot size attainable (w_0) by using the highest possible magnification available to us $(\times 100)$ and, hence, the largest $d\sigma/d\Omega$'s observed could be used (in principle) as representative of the longest tubes, which possibly span across the full length of the spot size. In turn, this allows us potentially to define a *differential cross section per unit length* of the tubes (which is then an intrinsic

property irrespective of their length).

Hence, except for the fact that part of the information is hidden in the statistical spread of signals, this is *not* a limitation to estimate the order of magnitude of an intrinsic $d\sigma/d\Omega$ and, in fact, the maximum measured cross sections should be a reliable estimate of how big the differential cross section per unit length can actually be for a specific wavelength (i.e. a specific resonance condition). For the rest of the study, we concentrate only on estimations of $d\sigma/d\Omega$'s for the particular case of RBM's.

Undoubtedly, an important breakthrough in the spectroscopy of carbon nanotubes came with the realization that *individual* nanotubes could be observed.[12] This automatically provides a recipe for the quantification of Raman cross sections. As pointed out before, the unequivocal signature of individual single-wall carbon nanotubes grown on a Si substrate could be observed through their different radial breathing modes (RBM's)[12] (see Figure 1). It is then possible to obtain an estimation of single nanotube differential Raman cross sections if we add an additional calibration (provided in the present study). We shall show explicitly here how this procedure can be performed, before moving on to a more direct measurement on our own samples.

Figure 1 (adapted from Ref.[12]) demonstrates the presence of individual nanotubes at different positions in the sample by observing the presence of distinct radial breathing modes (RBM's), in a similar fashion as the bi-analyte method used for single-molecule detection in SERS.[19] The particular three individual nanotubes in Figure 1 have been labeled by their different chiralities (specified by the numbers $(n,m) = (20,2), (11,11)$ and $(10,5)$, after Ref.[12]). These measurements have been performed in air, using a 785 nm laser with 25 mW (spot size $\sim 1\,\mu\mathrm{m}^2$). Each of the peaks gives an effective differential cross section for each individual tube. The trick is to link these values to a compound with a known differential cross section. For these particular results, this can be achieved using the second order Raman peak of Si at $\sim 303\,\mathrm{cm}^{-1}$ as a common reference. This Raman peak is *fully symmetric* (belonging to the Γ_1 irreducible representation of the point group of the crystal[20]) and, hence, this minimizes potential problems with the polarization dependence of the signal according to exact crystal orientation with respect to the incident polarization. This

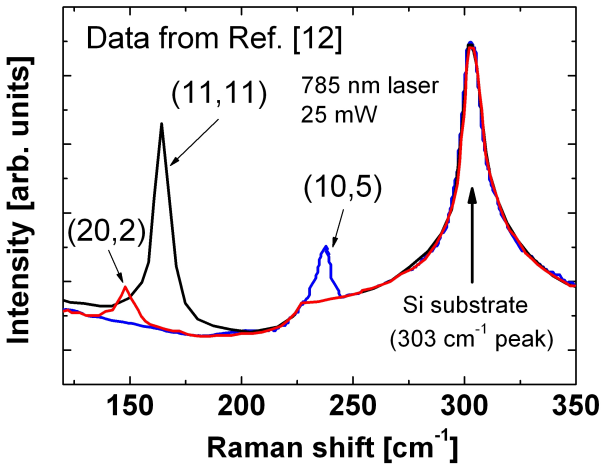

Figure 1: Individual single-walled carbon nanotubes data (reproduced from Fig. 2 in Ref.[12]). According to Ref.,[12] these data correspond to individual nanotubes with different chiralities (specified by the numbers:$(n,m) = (20,2), (11,11)$ and $(10,5)$, respectively). The spectra were taken on nanotubes grown by chemical vapor deposition on a Si substrate, with nanometer size iron catalyst particles (that act as a seed to start the growth). The sample had a density of ~ 6 nanotubes/μm^2 and the Raman spectra were taken with a 785 nm laser (1 μm^2 spot size, 25 mW laser power; see Ref.[12] for further details). The second order Raman peak of Si at $\sim 303\,\mathrm{cm}^{-1}$ is readily observable in the data, and links to our calibration of Raman differential cross sections.

Table 1: Summary of the RBM differential Raman cross-sections inferred from data of Ref.[12]

(n,m)	(20,2)	(11,11)	(10,5)
$\frac{d\sigma}{d\Omega}$[cm^2/sr]	3.28×10^{-23}	2.7×10^{-22}	4.1×10^{-23}

calibration requires a comparison of the Si Raman signal with a Raman cross-section standard (nitrogen gas here) and a careful characterization of the scattering volume. This procedure is detailed in Sec. S1 of the supplementary information. The results for the three RBM's in Figure 1 from the data in Ref.[12] are summarized in Table 1. Single nanotube differential Raman cross-sections range from 3×10^{-23} to $3\times10^{-22}\,\mathrm{cm}^2/\mathrm{sr}$ (depending on the specific nanotube).

Obviously, this two-step estimation via an intermediate reference (the Si Raman peak) is not the best method, but it demonstrates how Raman cross-sections may be estimated from existing nanotube data. We now describe a more direct measurement where Raman signals from individual nanotubes are directly compared to a Raman standard. For practical reasons, these experiments were carried out in slightly different samples (isotopically edited nanotubes) and at a different wavelength (633 nm). The details of the nanotube fabrication and sample preparation are given in

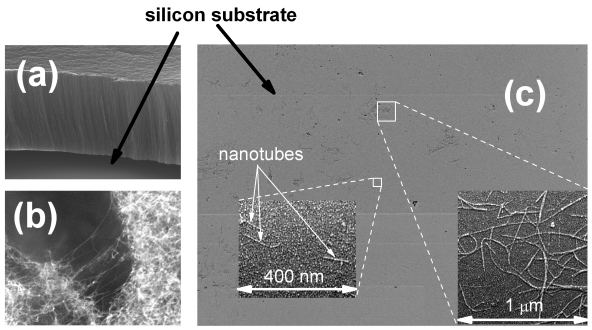

Figure 2: (a) Lateral SEM view of a forest of ^{13}C nanotubes on a Si substrate.[13,14] The tubes raise above the substrate to a height of $\sim 20\,\mu$m. (b) A closer look at much higher magnification ($\times$50K) reveals a dense mat of entangled tubes. The dark "gap" in the figure is ~ 100 nm accross. (c) General overview of the sample with dried nanotubes on Si (after dispersion, drying on Si, and repeated washings with water and ethanol). The two blown-up regions show multiple nanotubes (on the right) and isolated ones (on the left). Our final samples for Raman consist of regions of medium densities of tubes ($\sim 30-50$ nanotubes/μm^2) and regions of much smaller densities ($\sim 0-5$ nanotubes/μm^2). Undoubtedly some parts of the sample still contain bundles of tubes. But many regions contain objects that can be classified as *single tubes* (as far as the resolution of SEM allows). There is an additional "filter" in the number of tubes that are selected to be seen in the Raman spectra at each point, i.e.: the resonance condition with the laser (633 nm). This reduces further the effective number of tubes that are observable within the laser spot (beam waist of ~ 450 nm; see Fig. S2). Typical Raman spectra taken on this sample are shown in Figure 3

Sec. S2 of the Supplementary Information. Examples of SEM-images of our samples at different stages are shown in Figure 2. In the final samples for Raman, some regions contain clear evidence of multi-branched structures which are obviously bundles not fully separated in the centrifugation process, while other "sparser" areas show clear evidence for smaller (isolated) straight tubular structures of $\sim 100-300$ nm in length; attributed to individual nanotubes. SEM is (unfortunately) incapable to resolve the real diameter of these structures to confirm that they are individual nanotubes, but this is where the selectivity of RBM's in Raman spectroscopy comes into play.

We performed Raman mappings with a 633 nm laser (3 mW) in a Jobin-Yvon LabRam spectrometer attached to a BX41 Olympus optical microscope with a $\times$100 objective (indexed matched to air, NA=0.9). The differential cross sections for this laser line are going to be calibrated with respect to the differential cross section of the $\sim 2331\,$cm^{-1} mode of nitrogen gas (in air) at 633 nm. The results of the scattering volume characterization are summarized in Fig. S2 of the supplementary information. In Figure 3, we show several spectra selected from 3 different maps with

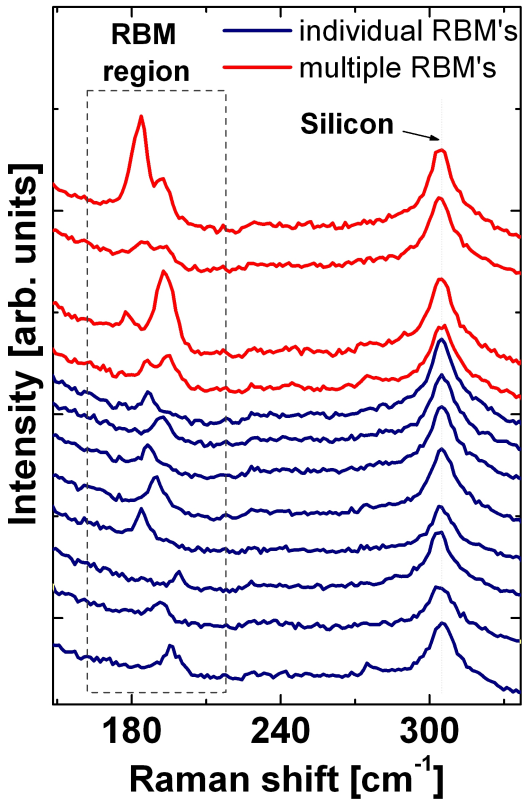

Figure 3: Selected spectra (out of 3 maps with 40×40 spectra) showing the unequivocal presence of RBM's corresponding to individual nanotubes. The spectra were taken with 3 mW @ 633 nm and 10 sec integration time with the ×100 objective. We scan areas on the sample that look mostly "clean" from the perspective of an optical microscope with a ×100 objective. Those areas are the ones that show the largest chance of detecting individual RBM's. Most of the time, the signal is simply that of the substrate. For these (isotopically edited) nanotubes the RBM's region is shown in a "box" in the figure. We show several examples of RBM's with different frequencies (blue), and we also show the presence of (every so often) spectra containing more than one type of RBM (red).

40×40 points (separated by 1 μm each (4800 spectra in total). We found approximately ~ 70 clear cases of spectra with single RBM's (with frequencies fluctuating in the RBM region for this tubes; $\sim 160-210\,\mathrm{cm}^{-1}$), and ~ 100 clear events with multiple nanotubes. A few examples of both cases are shown in Figure 3. The RBM's that are singled out as coming from individual nanotubes (blue spectra in Figure 3) can be directly compared with the nitrogen calibration differential cross section in Fig. S2 (accounting for the difference in integration times, while the power is kept constant at 3 mW). The analysis of the statistics of single nanotube signals and their differential cross sections is presented in Figure 4. We obtain differential cross sections for RBM's in the range:

$$\left(\frac{d\sigma}{d\Omega}\right)^{633\,\mathrm{nm}}_{\mathrm{RBM's}} \sim 1-4\times10^{-22}\,\mathrm{cm}^2/\mathrm{sr}\ \ (\text{on silicon}). \tag{1}$$

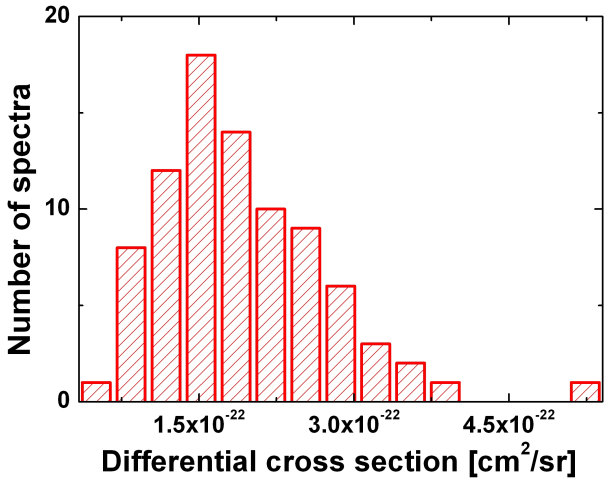

Figure 4: Histogram of differential Raman cross sections of individual RBM's of single nanotubes on Si from our Raman maps.

With all the provisos in mind of the experimental limitations to the (normally very difficult) problem of estimating $d\sigma/d\Omega$'s, we can conclude from this study that the experimental determination of differential cross sections for single nanotubes is indeed possible. Moreover, the two results from the two completely independent experiments can be considered to be in good agreement within experimental errors. Small differences can arise for a variety of reasons. For a start, the tubes in Ref.[12] are not the same type of tubes as we are measuring in our sample; and they are pos-

sibly larger (on average) than ours. In addition, there could be both a different resonance condition at 785 nm (expected), and an inaccurate estimation of the spot size (which was not the main point in Ref.[12] and, therefore, it is not estimated through a beam profiling method, like we do in the supplementary information of this paper). One way or another, we believe that both results show a consistent estimation of resonant differential cross sections in the range $4\times10^{-23}-4\times10^{-22}\,\mathrm{cm^2/sr}$, both at 633 nm and 785 nm excitation. It should be noted that these values apply to those nanotubes that were most resonant with the laser excitation, amongst a larger population.

Moreover, these values relate to the special case of *nanotubes on silicon*. If the same tubes were measured in vacuum or in a solvent, some corrections would arise. Firstly, the Si/air interface modifies the local electromagnetic environment, thereby affecting the Raman cross-section. This is the equivalent of the *enhancement factor* of SERS[16] and can be estimated in a first approximation from the Fresnel coefficients of the Si/air interface to be $F\sim(4/(n+1)^2)^2$, where n is the refractive index of Si. At 633nm or 785 nm (where $n\sim4$, mostly real[21]), it results in an enhancement factor correction on Si of $F\sim0.16$, i.e. the cross-section on Si should be approximately 6 times smaller than the one in vacuum. In a solvent, a local-field correction should also be applied.[16] For example, in water the Raman cross-section is expected to be ~2.5 larger than in vacuum.[16] Applying both the enhancement factor and local field correction, we can predict Raman cross-section as large as 6×10^{-21} cm^2/sr for RBM of the most resonant nanotubes in water. Finally, there may also be some chemical interaction of the nanotubes with the Si surface, which affects its electronic resonance and/or its Raman polarizability. Such effects are however difficult to quantify theoretically.

A natural question at this point is: how do these values compare with known differential cross sections of smaller resonant molecules? Although measuring resonant cross sections in dyes is a difficult task in general, the largest estimates of resonant differential resonant Raman cross sections are of the order of $\sim10^{-24}\,\mathrm{cm^2/sr}$ (for example for rhodamine 6G[22] in resonance at 532 nm laser excitation). The Raman cross-section of resonant nanotubes on Si are therefore a factor ~100 larger than those of resonant dyes (and possibly as much as ~1000 larger for nanotubes in water). These estimates should be useful for further theoretical investigations of the physical origin of the

large Raman cross-section of carbon nanotubes.

Finally, the large Raman cross-section of carbon nanotubes goes some ways in explaining why *single* carbon nanotubes can be detected by Raman spectroscopy. However, their cross-section remains smaller than typical SERS cross-sections required for single molecule detection of dyes with SERS.[16,17,23] The fact that they are "more visible" using Raman (with respect to resonant dyes) comes from the combination of two main factors: (i) they do not have problems with fluorescence, and (ii) they are incredibly robust against photobleaching (comparatively speaking), therefore allowing us to use long integration times and large laser power densities. No resonant dye would survive for an integration time of 10 sec with 3 mW of 633 nm laser under a $\times 100$ objective, as in Figure 3. Therefore, the detection of single dyes is considerably more difficult and needs to resort to additional amplification (i.e. SERS).

An important point of this study is that it rigorously quantifies the common view that resonant Raman cross sections of carbon nanotubes are "huge". We believe a proper estimation of the order of magnitude of differential cross sections of single nanotubes will contribute to the general understanding of the field, and will help to elucidate the real origin of other phenomena that has remained elusive in nanotubes, like vibrational pumping.

Acknowlegements

We are indebted to Shrividya Ravi (Victoria University of Wellington) for useful discussions and help with some of the samples. Special thanks are given to Olly Pantoja (Beaglehole Instruments, Wellington, NZ) for lending us a calibration lamp to test the response of our system.

Supporting Information Available

Details of the scattering volume characterization at 633 and 785 nm; method for using the apparent cross-section of the 303 cm^{-1} mode of Si to determine the Raman cross-section from published data; and further details on carbon nanotube and sample preparation.

References

(1) Reich, S.; Thomsen, C.; Maultzsch, J. *Carbon Nanotubes: Basic Concepts and Physical Properties*; Wiley-VCH: Berlin, 2004.

(2) Saito, R. *Physical Properties of Carbon Nanotubes*; World Scientific: Singapore, 2004.

(3) *Carbon Nanotubes: Advanced Topics in the Synthesis, Structure, Properties and Applications*; Jorio, A., Dresselhaus, G., Dresselhaus, M. S., Eds.; Springer: Berlin, 2008.

(4) Iijima, S. *Nature* **1991**, *354*, 56.

(5) Long, D. A. *The Raman effect, a unified treatment of the theory of Raman scattering by molecules*; John Wiley & Sons Ltd.: Chichester, 2002.

(6) Dresselhaus, M. S.; Pimenta, M. A.; Kneipp, K.; Brown, S. D. M.; Corio, P.; Marucci, A.; Dresselhaus, G. *in Science and Applications of Nanotubes*; Kluwer Academic/Plenum Publishers: New York, 2000.

(7) Lefrant, S.; Buisson, J.; Schreiber, J.; Wery, J.; Faulques, E.; Chauvet, O.; Baibarac, M.; Baltog, I. *in Spectroscopy of Emerging Materials*; Kluwer Academic Publishers: Amsterdam, 2004.

(8) Dresselhaus, M. S.; Eklund, P. C. *Advances in Physics* **2000**, *49*, 705.

(9) Saito, R.; Grüneis, A.; Samsonidze, G. G.; Brar, V. W.; Dresselhaus, G.; Dresselhaus, M. S.; Jorio, A.; Cancado, L. G.; Fantini, C.; Pimenta, M. A.; Filho, A. G. S. *New Journal of Physics* **2003**, *5*, 157.

(10) Filho, A. G. S.; Chou, S. G.; Samsonidze, G. G.; Dresselhaus, G.; Dresselhaus, M. S.; An, L.; Liu, J.; Swan, A. K.; Ünlü, M. S.; Goldberg, B. B.; Jorio, A.; Grüneis, A.; Saito, R. *Phys. Rev. B* **2004**, *69*, 115428.

(11) Kneipp, K.; Kneipp, H.; Dresselhaus, M. S.; Lefrant, S. *Philos. Trans. R. Soc. Lond. Ser. A-Math. Phys. Eng. Sci.* **2004**, *362*, 2361.

(12) Jorio, A.; Saito, R.; Hafner, J. H.; Lieber, C. M.; Hunter, M.; McClure, T.; Dresselhaus, G.; Dresselhaus, M. S. *Phys. Rev. Lett.* **2001**, *86*, 1118.

(13) Murakami, Y.; Chiashi, S.; Miyauchi, Y.; Hu, M.; Ogura, M.; Okubo, T.; Maruyama, S. *Chem. Phys. Lett.* **2004**, *385*, 298.

(14) Xiang, R.; Zhang, Z.; Ogura, K.; Okawa, J.; Einarsson, E.; Miyauchi, Y.; Shiomi, J.; Maruyama, S. *Jpn. J. Appl. Phys.* **2008**, *47*, 1971.

(15) Le Ru, E. C.; Etchegoin, P. G.; Meyer, M. *J. Chem. Phys.* **2006**, *125*, 204701.

(16) Le Ru, E. C.; Etchegoin, P. G. *Principles of Surface Enhanced Raman Spectroscopy and Related Plasmonic Effects*; Elsevier: Amsterdam, 2009.

(17) Le Ru, E. C.; Blackie, E.; Meyer, M.; Etchegoin, P. G. *J. Chem. Phys. C* **2007**, *111*, 13794.

(18) Duesberg, G. S.; Loa, I.; Burghard, M.; Syassen, K.; Roth, S. *Phys. Rev. Lett.* **2000**, *85*, 5436.

(19) Le Ru, E. C.; Meyer, M.; Etchegoin, P. G. *J. Phys. Chem. B* **2006**, *110*, 1944.

(20) Yu, P. Y.; Cardona, M. *Fundamentals of semiconductors: physics and materials properties*; Springer: Berlin, 2004.

(21) Etchegoin, P. G.; Kircher, J.; Cardona, M. *Phys. Rev. B* **1992**, *47*, 10292.

(22) Shim, S.; Stuart, C. M.; Mathies, R. A. *ChemPhysChem* **2008**, *9*, 6697.

(23) Etchegoin, P. G.; Le Ru, E. C. *Phys. Chem. Chem. Phys.* **2008**, *10*, 6079.

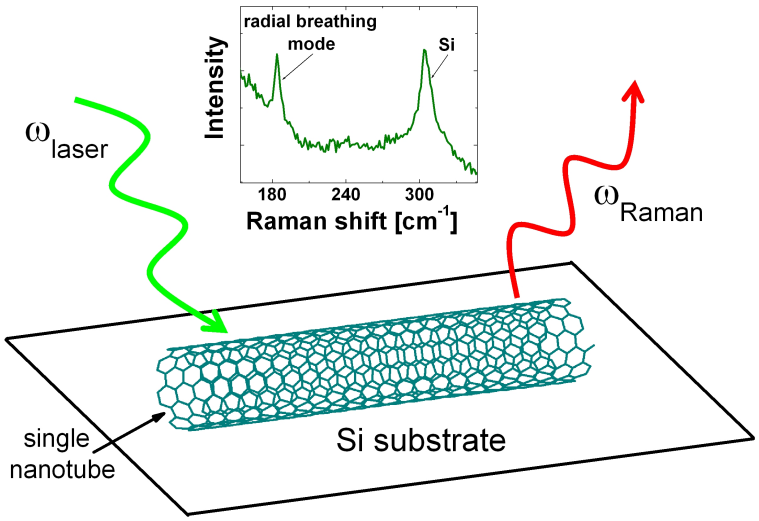

Figure 5: TOC figure.